Complexation of Np(V) with the dicarboxylates malonate and succinate: complex stoichiometry, thermodynamic data and structural information

Maiwald, M. M.; Müller, K.; Heim, K.; Rothe, J.; Dardenne, K.; Roßberg, A.; Koke, C.; Trumm, M.; Skerencak-Frech, A.; Panak, P. J.;

Originally published:

November 2021

Inorganic Chemistry 60(2021), 18674-18686

DOI: https://doi.org/10.1021/acs.inorgchem.1c01966

Complexation of Np(V) with the dicarboxylates malonate and succinate: complex stoichiometry, thermodynamic data and structural information

Martin M. Maiwald[1], Katharina Müller[3], Karsten Heim[3], Jörg Rothe[2], Kathy Dardenne[2], André Rossberg[3], Carsten Koke[1], Michael Trumm[2], Andrej Skerencak-Frech[2*], P. J. Panak[1,2]

1) Ruprecht Karls Universität Heidelberg, Physikalisch-Chemisches Institut, Im Neuenheimer Feld 253, 69120 Heidelberg, Germany
2) Karlsruher Institut für Technologie (KIT), Institut für Nukleare Entsorgung (INE), 76344 Eggenstein-Leopoldshafen, Germany
3) Helmholtz-Zentrum Dresden-Rossendorf, Institut für Ressourcenökologie, Bautzner Landstraße 400, 01328 Dresden, Germany

* E-Mail: andrej.skerencak@kit.edu

Abstract

The complexation of Np(V) with malonate and succinate is studied by different spectroscopic techniques, namely attenuated total reflection FT-IR (ATR FT-IR) and extended X-ray absorption fine structure (EXAFS) spectroscopy, as well as by quantum chemistry to determine the speciation, thermodynamic data and structural information of the formed complexes. For complex stoichiometries and thermodynamic functions (log β^0_n(T), $\Delta_r H^0_n$, $\Delta_r S^0_n$) near infrared absorption spectroscopy (Vis/NIR) is applied. The complexation reactions are investigated as a function of the total ligand concentration ($[Mal^{2-}]_{total}$, $[Succ^{2-}]_{total}$), ionic strength (I_m = 0.5 – 4.0 mol kg^{-1} $Na^+(Cl^-/ClO_4^-)$) and temperature (T = 20 – 85 °C). Besides the solvated NpO_2^+ ion, the formation of two Np(V) species with the stoichiometry $NpO_2(L)_n^{1-2n}$ (n = 1, 2, L = Mal^{2-}, $Succ^{2-}$) is observed. With increasing temperature the molar fractions of both complex species increase and the application of the law of mass action yields the temperature dependent conditional stability constants log $\beta`_n$(T) at given ionic strengths. The log $\beta`_n$(T) are extrapolated to IUPAC reference state conditions (I_m = 0) according to the specific ion interaction theory (SIT) revealing thermodynamic log β^0_n(T) values. For all formed complexes ($NpO_2(Mal)^-$: log β^0_1(25 °C) = 3.36 ± 0.11, $NpO_2(Mal)_2^{3-}$: log β^0_2(25 °C) = 3.95 ± 0.19, $NpO_2(Succ)^-$: log β^0_1(25 °C) = 2.05 ± 0.45, $NpO_2(Succ)_2^{3-}$: log β^0_2(25 °C) = 0.75 ± 1.22) the stability constants increase with

increasing temperature confirming an endothermic complexation reaction. The temperature dependence of the thermodynamic stability constants is described by the integrated Van't Hoff equation yielding the standard reaction enthalpies and entropies for the complexation reactions. In addition, the sum of the specific binary ion-ion interaction coefficients $\Delta\varepsilon_{0n}(T)$ for the complexation reactions are obtained from SIT modelling as a function of the temperature.

The structure of the complexes and the coordination mode of malonate and succinate are investigated using EXAFS spectroscopy, ATR-FT-IR spectroscopy and quantum chemical calculations. The results show, that in case of malonate 6-membered chelate complexes are formed, whereas the formation of 7-membered rings with succinate is energetically unfavourable in the equatorial plane of the Np(V) ion (as NpO_2^+ cation).

1 Introduction

As the long-term radiotoxicity of spent nuclear fuel is determined by long-lived radionuclides the geochemical behaviour of actinides (i.e. Np, Pu, and Am) is of particular interest in terms of nuclear waste disposal. For safety reasons the final emplacement of high-level nuclear waste in deep geological formations is the worldwide most preferred disposal option.[1-3] The intrusion of water into a nuclear waste repository is an important incident scenario which has to be considered for the safety case. Upon contact of the actinides with dissolved organic or inorganic ligands their (geo)chemical properties and migration behaviour can strongly be affected. [1, 4-19] In terms of nuclear waste disposal it is a key step to obtain a profound knowledge of the aqueous (geo)chemistry of the actinides including the most relevant interaction mechanisms, which is based on reliable thermodynamic data like standard stability constants $\log \beta^0(T)$ and standard enthalpies $\Delta_r H^0_m$ and entropies $\Delta_R S^0_m$ of reaction.

Independent of the host rock of the nuclear waste disposal, cementitious materials will be used for the construction of the geoengineered barriers. By adding superplasticizers (SP) the physical properties of cement and concrete are considerably improved. Regarding the interaction of SP with actinides, polycarboxylate-ether based macromolecules are of particular importance. [20-22] Due to their complex structure the characterization of their complexation properties toward actinide ions is challenging. In addition, the decomposition of macromolecular organic compounds will lead to the formation of various smaller carboxylic ligands with different structures, which can also be released from the cementitious materials. Thus, simple and defined carboxylic ligands (e.g. oxalate, malonate, succinate, salicylate, phthalate) are used as reference systems for the organic macromolecules and their degradation products to study the complexation properties of polycarboxylate ligands toward actinides.

In the last few years the complexation properties of trivalent actinides (An(III)) and lanthanides with model systems like oxalate, malonate or succinate and with commercially available superplasticisers have been studied extensively.[23-27] However, thermodynamic data for pentavalent actinides (An(V)) are scarce.

In the present work the formation and structure of Np(V)-malonate and -succinate complexes are studied and compared with the data for Np(V)-oxalate complexes. These ligand systems are the simplest dicarboxylic ligands with terminal COO^- groups and an increasing C-atom backbone from C_2 – C_4. This allows the characterisation of steric effects and the effect of multiple functional groups on the complex stability, thermodynamic behaviour and structure of An(V) complexes with organic ligands.

2 Experimental

Caution! *^{237}Np is a radioactive α-emitter and must be handled with care in laboratories appropriate for handling transuranic elements. Radiation exposure or incorporation causes health risks!*

The molal concentration scale (mol kg^{-1} H_2O^{-1} = mol kg^{-1}) was chosen for preparation of all solutions to avoid changes of the concentration based on changes of the temperature or ionic strength. All chemicals except for neptunium were reagent grade or higher and purchased from Merck Millipore or Alfa Aesar. All solutions and samples were prepared using ultrapure water (Milli-Q academic, Millipore, 18.3 MΩ cm).

2.1 Sample Preparation

For absorption spectroscopic measurements the total initial Np(V) concentration $[NpO_2^+]_{total}$ was set to 2.5 x 10^{-4} mol kg^{-1} in H_2O by dilution of a 6.1 x 10^{-2} mol kg^{-1} ^{237}Np(V) stock solution with 3.47 x 10^{-3} mol kg^{-1} $HClO_4$. Details on the preparation of the stock solution are given in the literature.[28] In all Np(V) sample solutions the total proton concentration $[H^+]_{total}$ was adjusted to 4.9 x 10^{-5} mol kg^{-1} with a standardized 0.02 mol kg^{-1} $HClO_4$. For determination of the complex stoichiometry the complexation of Np(V) with malonate (Mal^{2-}) and succinate ($Succ^{2-}$) was studied at a fixed ionic strength (I_m = 1.0 mol kg^{-1}) as a function of the total ligand concentration ($[Mal^{2-}]_{total}$ = 0 – 7.0 x 10^{-2} mol kg^{-1}; $[Succ^{2-}]_{total}$ = 0 – 8.1 x 10^{-2} mol kg^{-1}) and temperature (T = 20 – 85 °C). The ligand concentrations were increased by successive addition of portions of a 0.34 mol kg^{-1} Na_2Mal solution, respective Na_2Succ solution. The effect of the ionic strength and background electrolyte on the complexation is studied in NaCl and $NaClO_4$ media. The concentration of the background electrolytes was varied between $[NaCl]_{total}$ = 0.5 – 4.3 mol kg^{-1} and $[NaClO_4]_{total}$ = 0.5 – 2.4 mol kg^{-1} at fixed ligand concentrations ($[Mal^{2-}]_{total}$ = 2.1 x 10^{-3}, 2.3 x 10^{-2} mol kg^{-1}; $[Succ^{2-}]_{total}$ = 1.1 x 10^{-1}, 1.6 x 10^{-1} mol kg^{-1}). The concentration of $NaClO_4$ was increased by successive titration with an aqueous 14.1 mol kg^{-1} $NaClO_4$ solution. The amount of NaCl was increased by addition of solid NaCl to the samples. The total proton concentration in all titration

solutions was equal to that of the Np(V) samples. The total concentrations are defined as $[H^+]_{total} = [H^+]_{eq} + [HL^-]_{eq} + 2x\ [H_2L]_{eq}$ and $[L^{2-}]_{total} = [L^{2-}]_{eq} + [HL^-]_{eq} + [H_2L]_{eq} + [NaL^-]_{eq}$ (L = Mal, Succ).

2.2 Vis/NIR absorption spectroscopy

The complexation of Np(V) with malonate and succinate in aqueous solution was studied by Vis/NIR absorption spectroscopy between 20 and 85 °C. A Varian Cary 5G UV/Vis/NIR spectrophotometer in combination with a Lauda Eco E100 thermostatic system to control the temperature of the sample holder was used. The cuvettes (quartz glass, 1 cm path length, Hellma Analytics) were conditioned for 15 min at each temperature (10 °C step size) in a custom-made copper sample holder before measurement to ensure chemical equilibrium. The spectra were recorded between 950 – 1050 nm with a data interval of 0.1 nm, a scan rate of 60 nm min^{-1} (average accumulation time 0.1 s) and a slit width of 0.7 nm in double beam mode. For baseline correction identical samples without Np(V) were measured.

2.3 ATR-FT-IR spectroscopy

A Bruker Vertex 80/v vacuum spectrometer equipped with a mercury cadmium telluride (MCT) detector was used for FT –IR measurements. The spectra were recorded between 4000 and 600 cm^{-1} with a spectral resolution of 4 cm^{-1}. The ATR unit (DURA SamplIR II, Smiths Inc.) is a horizontal diamond crystal with nine internal reflections on the upper surface and an angle of incidence of 45°. A 200 µL flow cell was used to ensure adequate background subtraction without external thermal interference. The measurements were based on the principle of reaction-induced infrared difference spectroscopy. Further experimental details are given elsewhere. [29]

In situ ATR FT-IR spectroscopic measurements of the formed NpO_2^+ malonate and succinate complexes were performed in D_2O (Sigma Aldrich, 99.9 atom % D). This is due to the characteristic vibrational modes of the NpO_2^+ ion in solution that are generally detected below 850 cm^{-1} where strong interferences with modes of the bulk water (H_2O) occur. [30] All samples were prepared under inert gas atmosphere (N_2) to reduce the content of H_2O. The total NpO_2^+ concentration was 2.0 x 10^{-3} mol kg^{-1} (malonate) or 1.0 x 10^{-3} mol kg^{-1} (succinate). The ionic strength was I_m = 1.0 mol kg^{-1} (Na^+, Mal^{2-}/$Succ^{2-}$/Cl^-). NaCl was used as background electrolyte as it does not absorb light in the infrared region of interest. The total concentrations of malonate and succinate were $[Mal^{2-}/Succ^{2-}]_{tot}$ = 1.0 x 10^{-1} mol kg^{-1}. The pD_c between 4.0 and 7.4 was adjusted by addition of small aliquots of 0.2 or 2 mol l^{-1} DCl and 0.2 mol l^{-1} NaOD. For preparation of the respective acids and bases 35 wt. % DCl (Sigma Aldrich, 35 wt. % in D_2O, ≥ 99 atom % D) and 40 wt. % NaOD (Alfa Aesar, 40 wt.% in D_2O, 99.5 atom % D) and D_2O were used. The pD_c values were corrected according to pD = pH + 0.4. [31] Details on the definition of the conditional pH_c/pD_c values are given in the literature.[32, 33] The NpO_2^+ concentration and the species

distribution of the samples were confirmed after preparation by Vis/NIR spectroscopy using a Varian Cary 5G spectrometer connected directly to the N_2 glove box via optical fibres.

2.4 EXAFS measurements

The Np-L_3-edge-EXAFS measurements were performed at the INE-Beamline of the *Karlsruhe Research Accelerator, KARA, at* the *Karlsruhe Institute of Technology (KIT)* and the Rossendorf-Beamline (ROBL) at the *European Synchrotron Radiation Facility (ESRF)* in Grenoble.[34-38] All EXAFS spectra were recorded in fluorescence mode at 90 ° to the incident beam. At the INE-Beamline a 4 element Si SDD Vortex (SIINT) fluorescence and a 1 element Si Vortex-60EX SDD (SIINT) fluorescence detector were used. The ROBL-Beamline was equipped with a 13-element Ge-detector (Canberra). Details on the technical equipment and optical components of the beamlines are given in the literature. [34-38] Both beamlines were equipped with a double crystal monochromator (DCM) detuning the peak flux intensity in the middle of the scan range to 70%. Within the EXAFS range, the measurements were performed at equidistant *k*-steps. The integration time was increased with a $\sqrt{2}$ progression. The data were evaluated with the software packages EXAFSPAK, Athena -Demeter 0.9.26, and Artemis - Ifeffit 0.8.012.[39-41] Crystal structures of UO_2-malonate and UO_2-succinate were used for calculation of the theoretical scattering phases and amplitudes using FEFF8.40 and replacing U by Np.[42-45] The k^2- and k^3-weighted raw EXAFS spectra were used for data evaluation.

2.5 Quantum chemical calculations

Structure optimizations of the Np(V) malonate and succinate complexes were performed on density functional theory (DFT) level using the program package TURBOMOLE 7.0.[46] The BH-LYP functional was chosen for its better convergence compared to other hybrid-functionals. All C, O and H atoms were represented by basis sets of triple zeta basis quality (def-TZVP) and were treated at the all-electron level.[46, 47] The metal ion was represented by a 60-electron core pseudo-potential (Np, ECP60MWB) with corresponding basis sets of triple-zeta quality.[48] The complexes with different coordination modes (end-on vs. side-on) of the ligand molecules were optimized. The gas phase energies E_g of the triplet ground states were computed on the MP2 level. For a theoretical approximation of the Gibbs free energies G calculations of thermodynamic corrections ($E_{vib} = E_{zp} + H_0 - TS$, E_{zp} being the zero-point energy, H_0 and S are the enthalpy and entropy obtained from calculations of the vibrational modes) and solvation energies E_{solv} (obtained using COSMO, r_{Np} = 1.72 Å) were performed. The Gibbs free energies were calculated as follows: $G = E_g + E_{vib} + E_{solv}$. [49-51] Due to the ionic form of the Np(V) complexes a full second hydration shell was added and optimized to avoid the charge of the complexes to contact the COSMO cavity.

3 Results and Discussion

3.1 Vis/NIR absorption Spectroscopy

3.1.1 Absorption Spectra

The absorption spectra of Np(V) as a function of the total ligand concentration ($[Mal^{2-}]_{total}$, $[Succ^{2-}]_{total}$) at 20 and 85 °C are displayed in figure 1. The absorption band of the NpO_2^+ aquo ion at 20 °C and $I_m(NaClO_4)$ = 1.0 mol kg^{-1} is located at 980.1 ± 0.1 nm with a molar attenuation coefficient of $\varepsilon_{20\,°C}$ = 396 ± 4 L mol^{-1} cm^{-1}. This is in excellent agreement with literature data.[52-55] With increasing ligand concentration a bathochromic shift of the absorption band is observed for both ligand systems. In case of malonate the bathochromic shift accompanies the formation of two additional absorption bands at 988.0 ± 0.1 nm and 994.1 ± 0.2 nm. This indicates that two NpO_2^+ malonate complexes are formed. With increasing succinate concentration the bathochromic shift is less pronounced and only a broadening of the absorption spectrum is observed. The Full width at Half Maximum (FWHM) increases from 7.4 nm to 12.4 nm. In addition, one isosbestic point at 983.1 ± 0.2 nm is observed indicating the formation of one Np(V) succinate complex species. At 85 °C the spectrum of the NpO_2^+ aquo ion shifts hypsochromically by 1.6 nm and the molar attenuation coefficient decreases to $\varepsilon_{85\,°C}$ = 374 ± 10 L mol^{-1} cm^{-1}. With increasing ligand concentration a bathochromic shift is observed indicating the formation of NpO_2^+ complexes with malonate and succinate. In case of malonate the bathochromic shift at 85 °C is less pronounced compared to room temperature and the two absorption bands of the complex species are also hypsochromically shifted by about 1.3 nm. The smaller bathochromic shift indicates a hindered complexation of Np(V) with malonate at elevated temperatures. In contrast, for the complexation of Np(V) with succinate the FWHM at 85 °C increases to 13.2 nm with increasing $[Succ^{2-}]_{total}$ indicating a favoured complexation.

The temperature induced blue shift of the Np(V) absorption was already observed in previous studies.[54, 56-58] In the literature this effect was explained by changes of the physical properties (e.g. dielectric constant, refractive index, polarity) of water with increasing temperature affecting the electronic absorption of the NpO_2^+ ion.[54, 56] Also changes of the hydration in the first and second solvation sphere or changes of the complex geometries due to increasing temperatures might contribute to this shift.[57, 58]

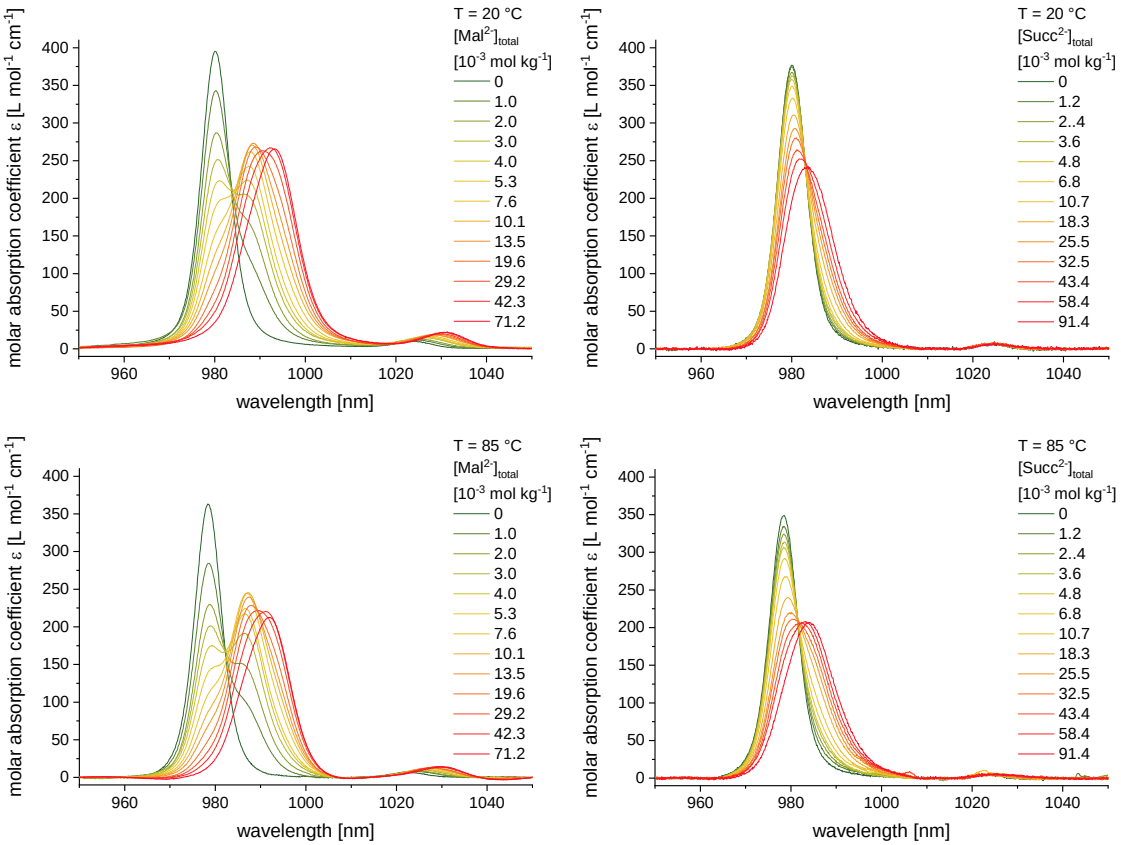

Figure 1: Absorption spectra of Np(V) with increasing malonate (left) and succinate (right) concentration at T = 20 (top) and 85 °C (bottom) and I_m(NaClO4) = 1.0 mol kg-1.

The temperature induced hypsochromic shift of the absorption band of the Np(V) ion is contrary to the bathochromic shift of the spectra resulting from the complexation of Np(V) with malonate and succinate. Due to this temperature dependency of the absorption bands, each series of spectra must be treated separately, and single component spectra must be determined for all studied experimental conditions.

3.1.2 Peak deconvolution

The single component spectra of the Np(V) complexes with malonate and succinate are derived via subtractive peak deconvolution. Details on this procedure are given elsewhere.[59] Identical spectra are

determined in NaCl and $NaClO_4$ media for the respective complex species at equal ionic strength. The single component spectra at 20 and 85 °C and $I_m(NaClO_4)$ = 1.0 mol kg^{-1} are displayed in figure 2.

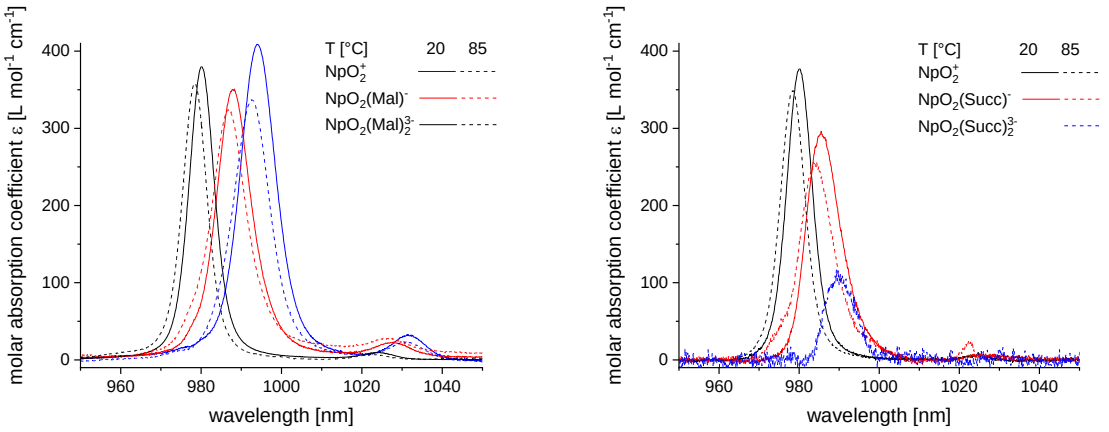

Figure 2: Absorption spectra of the solvated NpO_2^+ ion and the $NpO_2(L)_n^{1-2n}$ (n = 1, 2) (L^{2-} = Mal^{2-} (left), $Succ^{2-}$ (right)) complexes at T = 20 °C (solid lines) and 80° (dashed lines), $I_m(NaClO_4)$ = 1.0 mol kg^{-1}.

At 20 °C the single component spectra of two different NpO_2^+ malonate complex species display absorption bands at 988.0 ± 0.1 nm and 994.1 ± 0.2 nm which are hypsochromically shifted by 1.3 nm at 85 °C. In case of succinate only one absorption spectrum of a single NpO_2^+ succinate complex with an absorption maximum at 985.4 ± 0.1 nm is obtained at 20° C. At 85 °C the absorption band of this species is hypsochromically shifted by 1.7 nm and the absorption band of a second succinate complex with an absorption maximum at 989.7 ± 0.2 nm is observed. In table 1 the spectroscopic parameters of the NpO_2^+ complexes with malonate and succinate are summarized for 20 and 85 °C.

Table 1: spectroscopic properties of

T [°C]	complex	λ_{max} [nm]	ε_{max} [L mol^{-1} cm^{-1}]	λ_{FWHM} [nm]
20	NpO_2^+	980.1 ± 0.1	396 ± 4	7.4 ± 0.4
	$NpO_2(Mal)^-$	988.0 ± 0.1	365± 14	10.1 ± 0.5
	$NpO_2(Mal)_2^{3-}$	994.1 ± 0.2	425 ± 16	10.5 ± 0.6
	$NpO_2(Succ)^-$	985.4 ± 0.1	311 ± 5	9.9 ± 0.5
85	NpO_2^+	978.4 ± 0.1	374 ± 10	7.3 ± 0.4
	$NpO_2(Mal)^-$	986.7 ± 0.2	337 ± 13	10.4 ± 0.6
	$NpO_2(Mal)_2^{3-}$	992.6 ± 0.2	348 ± 14	10.8 ± 0.6
	$NpO_2(Succ)^-$	983.7 ± 0.2	269 ± 13	9.7 ± 0.5

	$NpO_2(Succ)_2^{3-}$	989.7 ± 0.2	117 ± 6	8.6 ± 0.4

Comparing the positions of the absorption bands of the malonate and succinate complexes shows that the complexation of NpO_2^+ with malonate results in a more pronounced bathochromic shift of approximately 7.3 nm for each coordinating ligand molecule compared to the complexation with succinate causing a bathochromic shift of only 5.6 nm per molecule. Furthermore, the effect of increasing temperature on the absorption bands of the malonate complexes is weaker compared to that of the NpO_2^+ succinate species.

3.1.3 Speciation and complex stoichiometry

The evolution of the different Np(V) malonate and succinate complexes as a function of the ligand concentration is derived by iterative deconvolution of the measured absorption spectra. Principle component analysis is applied using the single component spectra derived at each experimental condition (T, I_m). Details on this procedure are given in the literature.[59, 60] In figure 3 the experimental (symbols) and calculated (lines) species distributions are displayed as a function of the equilibrium malonate and succinate concentrations $[L^{2-}]_{eq}$ for T = 20 and 85 °C at $I_m(NaClO_4)$ = 1.0 mol kg^{-1}. At 20 °C the chemical equilibrium shifts towards the complexed Np(V) species with increasing ligand concentration and the formation of two malonate complexes and one succinate complex is observed. Furthermore, higher ligand concentrations and/or higher temperatures are required for succinate to form the two different complex species. This indicates a weaker complexation of Np(V) with succinate then with malonate. At 85 °C the speciation shifts to lower ligand concentrations for both ligand systems indicating an endothermic complexation behaviour.

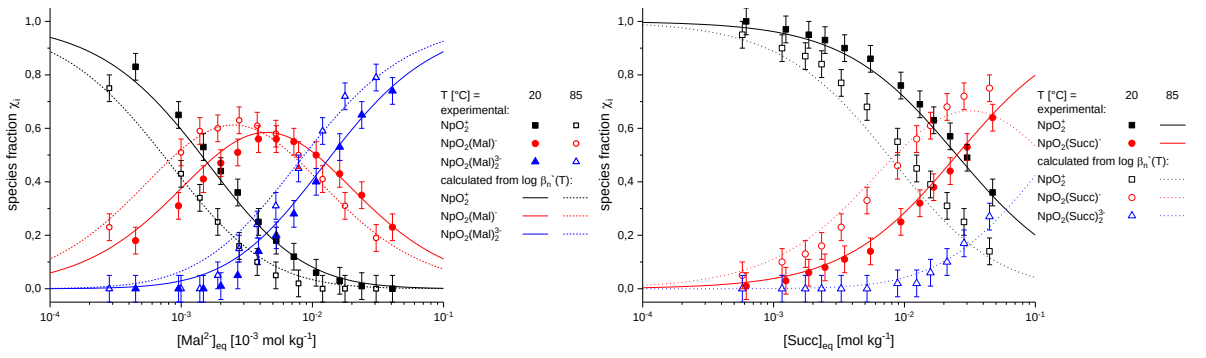

Figure 3: Experimentally determined (symbols) and calculated species distribution of the $NpO_2(L)_n^{1-2n}$ (n = 0, 1, 2; L^{2-} = Mal^{2-}, $Succ^{2-}$) complexes as a function of the equilibrium ligand concentration in aqueous solution. I_m = 1.0 $NaClO_4$; T = 20 °C (solid lines) and 85 °C (dashed lines).

The stoichiometry of the formed Np(V) malonate and succinate complexes is determined by slope analyses. The following complexation model (equation (1)) is used:

$$NpO_2^+ + L^{2-} \rightleftharpoons NpO_2(L)^-$$
$$NpO_2(L)^- + L^{2-} \rightleftharpoons NpO_2(L)_2^{3-} \quad (1)$$
$$\vdots$$
$$NpO_2(L)_{n-1}^{1-(2n-1)} + L^{2-} \rightleftharpoons NpO_2(L)_n^{1-2n}$$

The logarithmic form of the law of mass action for the stepwise complex formation according to equation (1) is given in equation (2):

$$\log K'_n = \log \frac{[NpO_2(L)_n]^{1-2n}}{[NpO_2(L)_{n-1}]^{1-(2n-1)}} - 1 \cdot \log[L^{2-}]_{eq}; \quad \beta'_n = \prod K'_n \quad (2)$$

with $[L^{2-}]_{eq}$ being the free, deprotonated malonate or succinate concentration in solution at a given temperature and ionic strength. Plots of $\log \frac{[NpO_2(L)_n]^{1-2n}}{[NpO_2(L)_{n-1}]^{1-(2n-1)}}$ versus $\log[L^{2-}]_{eq}$ are expected to yield a slope of one for each complexation step. For calculation of the equilibrium ligand concentration the protonation reactions of malonate and succinate and the formation of Na^+ complexes have to be considered:

$\log \beta_{A1}$: $L^{2-} + H^+ \rightleftharpoons HL^-$

$\log \beta_{A2}$: $HL^- + H^+ \rightleftharpoons H_2L$ (3)

$\log \beta_{Na}$: $L^{2-} + Na^+ \rightleftharpoons NaL^-$

The equilibrium concentrations of L^{2-}, HL^-, H_2L, NaL^-, H^+ are calculated with the software package Hyperquad Hyss2008, Version 4.0.31, as a function of $[L^{2-}]_{total} = [L^{2-}]_{eq} + [HL^-]_{eq} + [H_2L]_{eq} + [NaL^-]_{eq}$, $[H^+]_{total} = [H^+]_{eq} + [HL^-]_{eq} + 2x[H_2L]_{eq}$, I_m and T.[61] The temperature dependent thermodynamic stability constants $\log \beta_x(T)$ of the reactions given in equation (3) are calculated with the integrated Van't Hoff equation using the data reported in the literature.[62-67] The ionic strength dependence is accounted for by the specific ion interaction theory (SIT) as recommended by the Nuclear Energy Agency – Thermodynamic Database (NEA-TDB).[68] The binary ion-ion interaction coefficients $\varepsilon_{j,k}$ are taken from the NEA-TDB.[68]

The slope analyses for 20 and 85 °C at I_m = 1.0 mol kg^{-1} are displayed in figure 4. The results show a linear correlation of $\log \frac{[NpO_2(L)_n]^{1-2n}}{[NpO_2(L)_{n-1}]^{1-(2n-1)}}$ versus $\log[L^{2-}]_{eq}$. The linear regression analyses reveal slopes between 0.9 ± 0.1 and 1.2 ± 0.2 at all experimental conditions for both ligand systems. Thus, the formation of two different NpO_2^+ complexes with malonate and succinate with stoichiometries of

$NpO_2(L)_n^{1-2n}$ and n = 1 ,2 is confirmed. In case of succinate the formation of $NpO_2(Succ)_2^{3-}$ can only be observed for T > 50 °C.

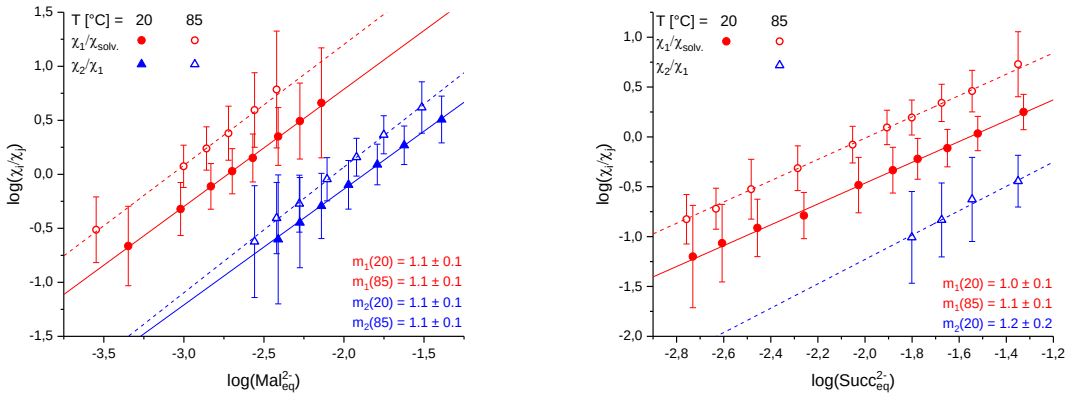

Figure 4: Plots of log ($[NpO_2(L)_n]^{1-2n}/[NpO_2(L)_{n-1}]^{3-2n}$) vs. log ($[L^{2-}]_{eq}$) and linear regression analyses at T = 20, 85 °C and I_m = 1.0 mol kg^{-1} H_2O. (left): L^{2-} = Mal^{2-}, (right) L^{2-} = $Succ^{2-}$.

3.1.4 Thermodynamic data

The determination of thermodynamic functions (log β^0_n(T), $\Delta_R H^0_{m,n}$, $\Delta_R S^0_{m,n}$) at IUPAC reference state conditions (I_m = 0, T = 298 K) requires conditional stability constants log β'_n(T) at various I_m and T. Therefore, log β'_n(T) values for the formation of $NpO_2(L)^-$ and $NpO_2(L)_2^{3-}$ are calculated according to the law of mass action (eqn. (2)) at various temperatures and NaCl or $NaClO_4$ concentrations. These data are extrapolated to I_m = 0 according to equation (4) yielding the thermodynamic stability constants log β^0_n(T).[68]

$$log\, K'(T) - \Delta z^2 D = log\, K^0(T) + \Delta\varepsilon I_m \qquad (4)$$

D is the Debye-Hückel term, $\Delta z^2 = \sum z^2_{end} + \sum z^2_{start}$ is the sum of the charges z and $\Delta\varepsilon = \sum\varepsilon_{end} + \sum\varepsilon_{start}$ is the sum of the binary ion-ion interaction coefficients $\varepsilon_{j,k}$ of the reactants. For both ligand systems a linear correlation of log β'_n(T) – $\Delta z^2 D$ versus I_m is observed for all studied temperatures. Equal log β^0_n(T) values are obtained for both electrolytes (NaCl, $NaClO_4$) as expected due to the application of the SIT (see ESI table S1 and table S2). Thus, averaged log β^0_n(T) values are calculated for the respective malonate and succinate complexes. The averaged log β^0_n(T) values are listed in table 2.

Table 2: Thermodynamic stability constants log β^0_n(T) for $NpO_2(L)_n^{1-2n}$ (n = 1, 2) with L^{2-} = Mal^{2-}, and $Succ^{2-}$ as a function of the temperature

T [°C]	Mal^{2-}	$Succ^{2-}$

$NpO_2^+ + L^2 \rightleftarrows NpO_2(L)^-$	20	3.31 ± 0.07	2.13 ± 0.15
	30	3.41 ± 0.08	2.11 ± 0.14
	40	3.42 ± 0.09	2.12 ± 0.10
	50	3.51 ± 0.08	2.19 ± 0.10
	60	3.50 ± 0.09	2.26 ± 0.12
	70	3.54 ± 0.08	2.36 ± 0.11
	80	3.56 ± 0.09	2.53 ± 0.20
	85	3.61 ± 0.08	2.56 ± 0.22
$NpO_2^+ + 2\,L^2 \rightleftarrows NpO_2(L)_2^{3-}$	20	3.90 ± 0.11	-
	30	3.99 ± 0.08	-
	40	4.04 ± 0.10	-
	50	4.20 ± 0.09	1.41 ± 0.21
	60	4.20 ± 0.14	1.67 ± 0.15
	70	4.25 ± 0.11	1.77 ± 0.16
	80	4.30 ± 0.11	2.00 ± 0.22
	85	4.35 ± 0.12	2.26 ± 0.24

In case of malonate an increase of log β^0_1(20 °C) = 3.31 ± 0.07 to log β^0_1(85 °C) = 3.61 ± 0.08 and of log β^0_2(20 °C) = 3.90 ± 0.11 to log β^0_2(85 °C) = 4.35 ± 0.12 is observed. For the complexation of Np(V) with succinate an increase of log β^0_1(20 °C) = 2.11 ± 0.14 to log β^0_1(85 °C) = 2.56 ± 0.22 and log β^0_2(50 °C) = 1.14 ± 0.21 to log β^0_2(85 °C) = 2.26 ± 0.24 is observed. Comparison of the results shows that the stability constants of $NpO_2(Succ)^-$ are by 1.1 – 1.2 logarithmic units lower compared to $NpO_2(Mal)^-$, whereas. the stability constants of $NpO_2(Succ)_2^{3-}$ are by 2.1 – 2.8 lower compared to those of the respective $NpO_2(Mal)_2^{3-}$-complex. These results confirm the observations that Np(V) forms weaker complexes with succinate than with malonate.

The determination of the standard reaction enthalpies $\Delta_r H^0_{n,m}$ and entropies $\Delta_r S^0_{n,m}$ of the respective complexation reactions is performed according to the integrated Van´t Hoff equation given in equation (5).[62]

$$\log \beta_n^0(T) = \log \beta_n^0(T_0) + \frac{\Delta_r H_{n,m}^0(T_0)}{R \ln(10)} \left(\frac{1}{T_0} - \frac{1}{T}\right) \quad (5)$$

R is the universal gas constant. In figure 5 the standard stability constants log β^0_n(T) are plotted versus the reciprocal temperature T^{-1}. The data show a linear correlation. The standard reaction enthalpies are obtained from the slopes of the linear regression analyses (log $\beta^0_n(T) = m \times T^{-1} + C$): $\Delta_r H^0_{n,m} = -m_n \times R \times \ln(10)$. The standard reaction entropies are calculated from the intercepts of the y-axis: $\Delta_r S^0_{n,m} = C \times R \times \ln(10)$.

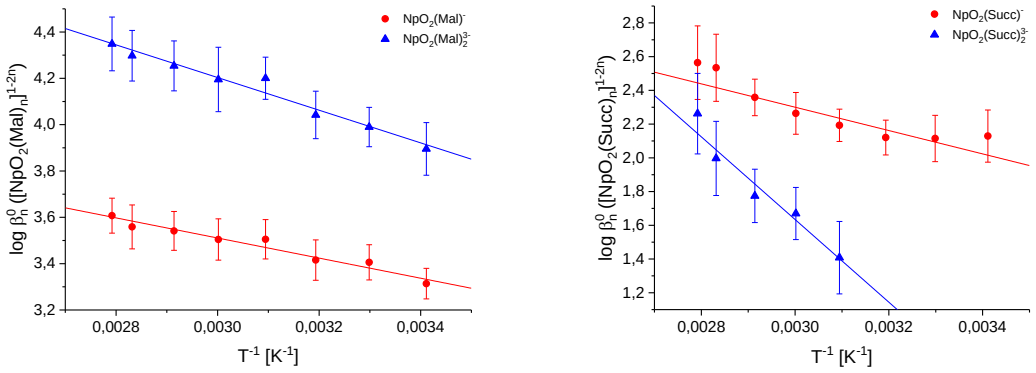

Figure 5: Plots of log β^0_n(T) (n = 1, 2) as a function of the reciprocal temperature and fittings according to the integrated Van´t Hoff equation.

All complexation reactions have positive $\Delta_r H^0_{n,m}$ values indicating an endothermic complexation driven by the gain of entropy. In table 3 the determined thermodynamic functions ($\Delta_r H^0_{n,m}$, $\Delta_r S^0_{n,m}$) and thermodynamic stability constants at 25 °C are summarized and compared to literature data.[69] The NIST standard reference database 46 version 8.0 lists thermodynamic stability constants for $NpO_2(Mal)^-$ and $NpO_2(Succ)^-$ which are in excellent agreement with the results of the present work. Unfortunately, no $\Delta_r H^0_{m,1}$ and $\Delta_r S^0_{m,1}$ values are given for these complexes.

To investigate steric effects the results for the Np(V) complexes of the present work are compared to recently published data for the complexation of Np(V) with oxalate.[70] Comparison of log β^0_n(T) of oxalate, malonate and succinate reveals a successive decrease of the complex stability with increasing C-backbone of the dicarboxylates. For $NpO_2(L)^-$ log β^0_1(25 °C) decreases by approximately 1.2 from oxalate to malonate and additionally by 1.3 from malonate to succinate. In case of $NpO_2(L)_2^{3-}$ the decrease is even stronger. From oxalate to malonate log β^0_2(25 °C) decreases by 2.3 and from malonate to succinate by 3.2 logarithmic units. A similar trend is observed for the standard reaction enthalpies. The formation of $NpO_2(Ox)_n^{1-2n}$ is exothermic, whereas the formation of $NpO_2(Mal)_n^{1-2n}$ is weakly endothermic and an additional increase of $\Delta_r H^0_{n,m}$ is observed for $NpO_2(Succ)_n^{1-2n}$. Our structural

investigations (see section below) show that these trends originate from changes in the coordination mode in the series oxalate, malonate, and succinate with the NpO_2^+ ion.

Table 3: Conditional stability constants for the complexation of Np(V) with oxalate, malonate and succinate at ionic strength I = 1.0 in $NaClO_4$ media and T = 25 °C.

Complex	log β^0_i(25 °C)	$\Delta_r H^0_{n,m}$ [kJ mol^{-1}]	$\Delta_r S^0_{n,m}$ [kJ mol^{-1}]	Ref.
$NpO_2(Ox)^-$	4.53 ± 0.12	-1.3 ± 0.7	83 ± 2	
$NpO_2(Ox)_2^{3-}$	6.22 ± 0.24	-8.7 ± 1.4	90 ± 5	
$NpO_2(Mal)^-$	3.36 ± 0.11	8.3 ± 0.7	92 ± 2	p.w.
	3.16			[69]
$NpO_2(Mal)_2^{3-}$	3.95 ± 0.19	13.5 ± 1.1	121 ± 3	p.w.
$NpO_2(Succ)^-$	2.05 ± 0.45	13.2 ± 2.7	83 ± 8	p.w.
	2.13			[69]
$NpO_2(Succ)_2^{3-}$	0.75 ± 1.22	47.0 ± 7.4	172 ± 22	p.w.

A: solvent extraction with thenoyl-trifluoroacetone (TTA) and 1,10-phenantroline (Phen); organic diluent: iso-butylmethyl-ketone. **R**: solvent extraction with TTA and alkylammonium. **sp**: spectrophotometry. **p.w.**: present work.

Additionally, the SIT modelling of the ionic strength dependence of log β'_n(T) reveals the sum of the binary ion-ion interaction coefficients $\Delta\varepsilon_{0n}$(T) as a function of the temperature for the background electrolytes NaCl and $NaClO_4$. In figure 6 the $\Delta\varepsilon_{0n}$(T) values are displayed as a function of the temperature for $NpO_2(Mal)_n^{1-2n}$ and $NpO_2(Succ)_n^{1-2n}$. In all systems no significant temperature dependence of $\Delta\varepsilon_{0n}$(T) is observed and averaged, temperature independent $\Delta\varepsilon_{0n}$ values are calculated (given as solid lines). This is in good agreement with the negligible T dependence of $\Delta\varepsilon_{0n}$(T) values for Np(V) and An(III) complexes with various organic and inorganic ligands described in the literature . [23, 32, 53, 54, 56, 71, 72]

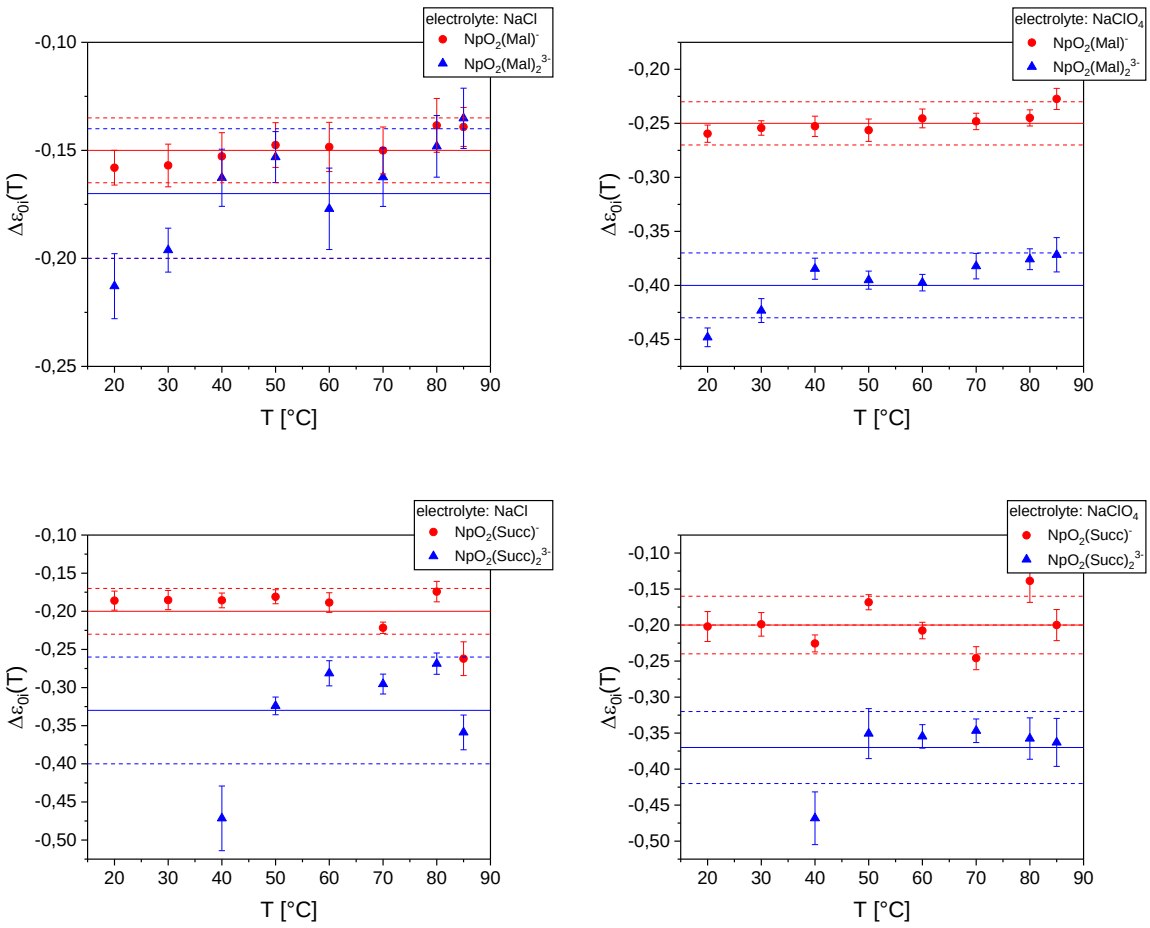

Figure 6: $\Delta\varepsilon_{j,k}(T)$ values for the formation of $[NpO_2(L)_n]^{1-2n}$ (n = 1, 2; L^{2-} = Mal^{2-}, $Succ^{2-}$) in NaCl (left) and $NaClO_4$ (right) as a function of the temperature. The error bars (dashed lines) equal the 1σ error of the mean value (dashed lines).

The binary ion-ion interaction coefficients $\varepsilon_{j,k}$ of the $NpO_2(L)_n^{1-2n}$ complexes (L^{2-} = Mal^{2-}, $Succ^{2-}$) with Na^+ are calculated according to the SIT using equation (6) and the interaction coefficients $\varepsilon(NpO_2^+, ClO_4^-)$ = 0.25 ± 0.05, and $\varepsilon(NpO_2^+, Cl)$ = 0.09 ± 0.05 given in the NEA-TDB. The values of $\varepsilon(Na^+, Mal^{2-})$ = -0.05 ± 0.03 and $\varepsilon(Na^+, Succ^{2-})$ = 0.09 ± 0.02 are calculated from literature data using the SIT procedure.[64, 73, 74]

$$\Delta\varepsilon = \sum \varepsilon_{products} - \sum \varepsilon_{educts} \qquad (6)$$

The $\varepsilon_{j,k}$ values are given in table 4. According to the SIT identic $\varepsilon_{j,k}$ values should be obtained for the respective complexes regardless of the used background electrolyte. This is not the case for $NpO_2(Mal)_n^{1-2n}$ and $NpO_2(Succ)_n^{1-2n}$ (n = 1, 2) as slight deviations are observed for the values determined in NaCl or $NaClO_4$ media. In previous studies it was shown that these discrepancies originate from a defective $\varepsilon(NpO_2^+, ClO_4^-)$ = 0.25 ± 0.05 reported in the NEA-TDB.[53, 56, 72, 73] Nevertheless, the log $\beta^0_n(T)$ of the respective complex species obtained in NaCl or $NaClO_4$ are in excellent agreement. Thus, the ionic strength dependence of log $\beta^0_n(T)$ is accurately described with the $\Delta\varepsilon_{0n}$ determined in this work.

Table 4: Temperature independent binary ion-ion interaction coefficients $\varepsilon_{j,k}$ for the formation of $NpO_2(L)_n^{1-2n}$ (n = 1, 2; L^{2-} = Mal^{2-}, $Succ^{2-}$) in NaCl and $NaClO_4$ media.

electrolyte	$NpO_2(Mal)^-$	$NpO_2(Succ)^-$	$NpO_2(Mal)^-$	$NpO_2(Succ)_2^{3-}$
NaCl	-0.12 ± 0.06	-0.02 ± 0.04	-0.20 ± 0.06	-0.06 ± 0.08
$NaClO_4$	-0.06 ± 0.04	0.14 ± 0.04	-0.27 ± 0.05	0.06 ± 0.06

3.2 Structure and coordination modes

The observed trends within spectroscopic properties and the thermodynamic data in the series Np(V)-oxalate, malonate, succinate are expected to originate from different coordination modes of the ligands towards the metal center (see scheme 1). Malonate and succinate can either coordinate with only one COO^- group towards the Np(V) ion (end-on; bidentate coordination with both O-atoms of one COO^- group) or they form chelate rings with both COO^- groups coordinating to the metal center (side-on; monodentate coordination with one O-atom of each COO^- group).

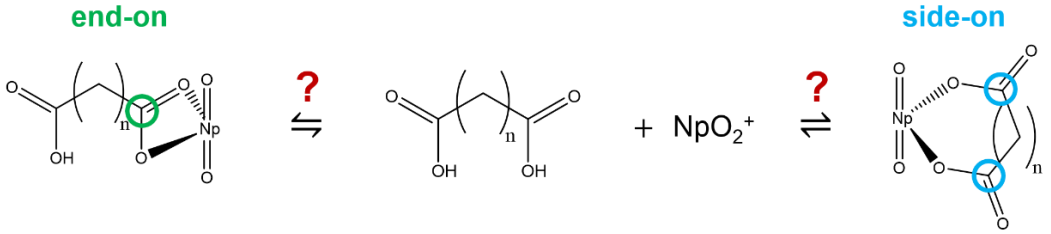

Scheme 1: Structures of the 1:1 Np(V) complexes with malonate (n = 1) and succinate (n = 2) with different coordination modes. left: end-on coordination with a bidentate coordinating COO^- group; right: side-on coordination with monodentate coordination of both COO^- groups.

3.2.1 ATR-FT-IR spectroscopy

Information on the coordination mode of Np(V) with dicarboxylic acids can be derived from the vibrational modes of the ligands and the NpO_2^+ ion. Prior to the analysis of the NpO_2^+ complexes, the vibrational absorption spectra of the dissolved ligands at selected pD values are recorded (Fig 7 top). At low pD values, the spectra of the free ligands show strong absorption bands at ~1700 cm^{-1}, which decrease with increasing pD and are not observed at neutral pD values. These bands are assigned to the stretching vibrational mode of the COOD groups of the dicarboxylic acids. Furthermore, bands between 1565 to 1580 cm^{-1} and between 1350 to 1410 cm^{-1} are observed. These bands represent the antisymmetric ($\nu_{as}(COO^-)$) and symmetric ($\nu_s(COO^-)$) stretching modes of the COO^- group, respectively.

The infrared spectra of the Np(V) complex species at pD values between 4.0 and 7.4 are shown in Fig. 7 (bottom). These difference spectra were calculated from single-beam spectra of the Np(V) complex solution and the free ligand solution at identical experimental conditions. As a result, constant parts

of the spectra, in particular the strong absorbing background from the bulk water, but also contributions from the experimental setup, are minimized. The complexation of Np(V) with malonate and succinate results in changes in the electron density distribution within the COO^--groups and the Np=O bonds leading to characteristic changes in the respective vibrational modes. These changes are observed as negative and positive bands in the difference spectra.

The negative absorption bands at ~1700 cm^{-1} in the spectra at low pD_c conditions are attributed to carboxyl groups of the uncomplexed malonic and succinic acids. Due to the complexation of the Np(V) ion with Mal^{2-} the protonation equilibrium of the ligand is shifted towards the deprotonated ligand species Mal^{2-}, which is reflected by the negative absorption band of the C=O stretching vibration at ~1700 cm^{-1}. This is verified by the difference spectrum calculated from spectra of the malonate ligand recorded at pD 7.4 and 4.7 (blue trace in Fig. 7) also showing a negative band in the frequency range >1350 cm^{-1}. Comparable results are obtained for succinate.

The positive bands at 1563 and 1362 cm^{-1} in the malonate spectra (Figure 7 bottom, left) and 1565, and 1397 cm^{-1} in the succinate spectra (Figure 7 bottom, right) represent modes of the carboxylate groups in the Np(V) complexes. For both ligands, a shift of the antisymmetric stretching mode $\nu_{as}(COO^-)$ to lower wavenumbers is observed. For malonate, the shift is 18 cm^{-1} from 1581 to 1563 cm^{-1}. For succinate, $\nu_{as}(COO^-)$ shifts about 11 cm^{-1} from 1565 to 1554 cm^{-1}. These spectral shifts indicate a change in the electron density within the COO^- group caused by the strong ionic character of the NpO_2^+ - ligand bond. In contrast, the frequency of the symmetrical stretching vibrational mode $\nu_{as}(COO^-)$ appears less sensitive with respect to the ionic interactions with Np(V), as the frequencies of these modes are observed in all spectra at 1362 and 1397 cm^{-1}.

An assignment of the coordination mode of the ligand to a complexing metal ion can be potentially derived from the spectral splitting of the $\nu_{as}(COO^-)$ and $\nu_s(COO^-)$ stretching modes. [76] The splitting of ~200 cm^{-1} in case of Np(V) -malonate suggests a monodentate coordination of the COO^- group to the Np(V) ion excluding an end-on coordination mode (see scheme 1). Consequently, the considerably lower splitting in the series of the Np(V)-succinate spectra indicates a different kind of coordination, namely an end-on coordination.

In addition to the vibrational modes of the ligands, the antisymmetric stretching vibrational mode ν_3(Np=O) gives valuable hints on the complex stoichiometry. For the free Np(V) ion it occurs at 820 cm^{-1}. [30, 77] Upon complex formation the band is considerably shifted to lower wavenumber, which is explained by the ionic character of Np(V) carboxylate bond resulting in a change of the charge density between Np and the axial O atoms.

Upon complexation with malonate at pD 4.7 and 5.2 a broad band is observed at around 790 cm^{-1}. The second derivative reveals two peaks at 801 and 783 cm^{-1} corresponding to the $NpO_2(Mal)_n^{1-2n}$ (n = 1, 2) complexes for this band. Upon increasing the pD up to 7.4, the band shows a symmetric shape centering at 783 cm^{-1} showing the predominance of $NpO_2(Mal)_2^{3-}$.

Upon complexation with succinate, ν_3(Np=O) is only slightly shifted by 4 cm^{-1} at pD 4.0. With increasing pD from 4.0 to 5.2 and finally 7.4 the band shows a bathochromic shift to 800 cm^{-1}. At pD 7.4, the symmetric shape of the ν_3(Np=O) bands suggest the predominance of one species which is assigned to $NpO_2(Succ)^-$.

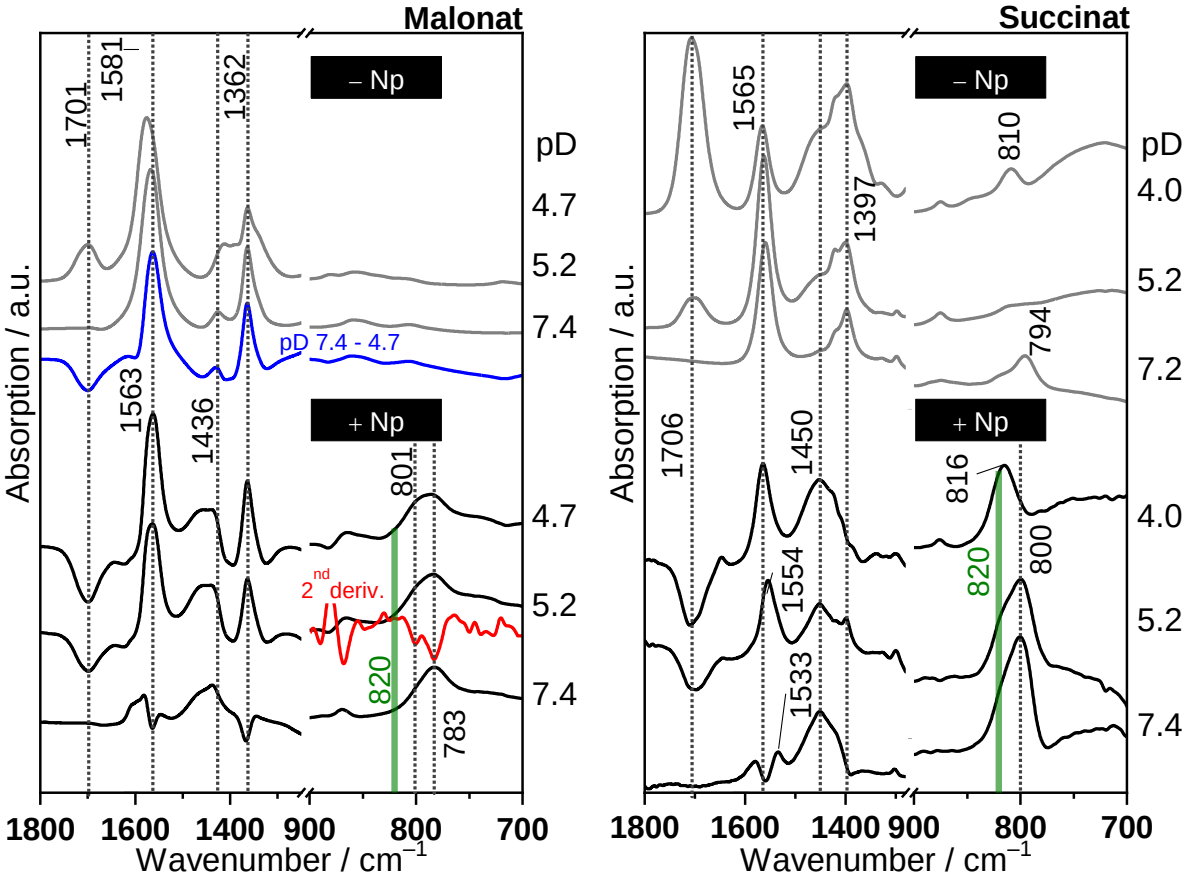

Figure 7: Mid-IR spectra of aqueous deuterated solutions of malonate (left) and succinate (right) in the absence (-Np) and presence (+Np) of Np(V) at different pD values ([Np]=2 mmol kg^{-1} (Mal^{2-}) and 1 mmol kg^{-1} for ($Succ^{2-}$), $[Mal^{2-}/Succ^{2-}]_{tot}$ = 0.1 mol kg^{-1}, I_m = 1.0 mol kg^{-1} (Na^+, $Mal^{2-}/Succ^{2-}/Cl^-$))

3.2.2 EXAFS spectroscopy

Information on the bond distances and the coordination mode of the ligands in the respective $NpO_2(L)_n^{1-2n}$ complexes are determined by EXAFS spectroscopy. Np-L_3-EXAFS spectra of Np(V) in the presence of malonate or succinate are recorded as a function of the pH_c value. The k^2-weighted Np-L_3EXAFS spectra, the Fourier Transformations and the fit curves are displayed in figure S1 and figure

S2 in the ESI. Detailed results and the respective fitting parameters are given in the ESI (table S3 and table S4). In table 5 the distances between the ligand atoms and the Np(V) center are summarized. The results show, that for the axial O-atoms (O_{ax}) of the Np(V) complexes an averaged distance of 1.84 ± 0.01 Å is obtained. For the equatorial O-atoms (O_{eq}) the average distance is 2.47 ± 0.02 Å and the coordination number in the equatorial plane counts for 3.5 – 5.1 through the series of samples. These results are in excellent agreement with literature data. [37, 78] The coordination mode of the dicarboxylates is determined using the distances of the C-atoms of the coordinating carboxylic groups C_c. For the malonate complexes the C_c distance is 3.41 ± 0.03 Å and for the succinate complexes 2.83 ± 0.04 Å. Thus, distinctively longer C_c distances are obtained for the $NpO_2(Mal)_n^{1-2n}$ complexes compared with $NpO_2(Succ)_n^{1-2n}$. This difference indicates different coordination modes. In the literature two C_c distances are reported for the Np(V)-acetate and -propionate complexes which are 2.91 ± 0.02 and 2.87 ± 0.03 Å.[32, 79] These monocarboxylic ligands coordinate via one COO^- group towards the Np(V) ion and thus these C_c distances serve as reference for an end-on binding mode. The present result for succinate is in excellent agreement with the data for the acetate and propionate complexes confirming an end-on coordination of succinate. In contrast the C_c distance in the malonate complexes are by 0.50- 0.58 Å longer indicating the formation of chelate rings involving one O-atom of each COO^- group. Furthermore, the C_c distance in the $NpO_2(Mal)_n^{1-2n}$ complexes is in excellent agreement with results for Np(V) oxalate complexes also displaying side-on coordination (C_c: 3.32 ± 0.06 Å).[70]

Table 5: Distances of the coordinating fist-shell O-Atoms and of the C-atoms of coordinating COO^- groups in the $NpO_2(L)_n^{1-2n}$ (n = 1, 2, L^{2-} = Mal^{2-}, $Succ^{2-}$) complexes obtained by EXAFS spectroscopy.

	Propionate[32]	Oxalate[xx]	Malonate [p.w.]	Succinate [p.w.]
O_{ax}	1.82(1)	1.83(1)	1.85(1)	1.83(1)
O_{eq}	2.471)	2.45(2)	2.48(2)	2.48(2)
C_c	2.87(3)	3.39(7)	3.41(4)	2.83(5)

3.2.3 Quantum chemical calculations

The experimentally determined coordination modes and structural data are supported by quantum chemical calculations. The structures of the fivefold $NpO_2(Mal)_n^{1-2n}$ and $NpO_2(Succ)_n^{1-2n}$ complexes (compare scheme 1) are optimized. In the equatorial plane of the complexes 3 or 1 water molecule for $NpO_2(L)^-$ or $NpO_2(L)_2^{3-}$ are added to obtain the coordination number of 5. In table 6 the results are summarized and compared with the experimentally determined distances. For both systems the O_{ax} and O_{eq} distances are in excellent agreement with the experimental results. Furthermore, the

calculations reveal a C_c distance for $NpO_2(Mal)_n^{1-2n}$ of 3.44 Å (n = 1) and 3.47 Å (n = 2) for side-on coordinating ligand molecules. This is in perfect accordance with the EXAFS results. In case of $NpO_2(Succ)_n^{1-2n}$ C_c distances of 2.86 Å (n = 1) and 2.92 Å (n = 2) are obtained hinting to an end-on coordination. Thus, the obtained distances from structure optimizations confirm the interpretation of the EXAFS results.

Table 6: Distances of the ligands atoms towards the Np(V) ion obtained from structure optimizations on DFT level and comparison with the EXAFS results.

method	complex	Coord.mod.	O_{ax} [Å]	O_{eq} [Å]	C_c [Å]
DFT	$NpO_2(Mal)^-$	end-on	1.82	2.49	2.88
		side-on	1.82	2.46	3.44
	$NpO_2(Mal)_2^{3-}$	end-on	1.82	2.48	2.90
		side-on	1.83	2.44	3.47
EXAFS	$NpO_2(Mal)^-$/ $NpO_2(Mal)_2^{3-}$		1.85 ± 0.01	2.48 ± 0.02	3.41 ± 0.04
DFT	$NpO_2(Succ)^-$	end-on	1.81	2.47	2.86
		side-on	1.82	2.46	3.49
	$NpO_2(Succ)_2^{3-}$	end-on	1.80	2.51	2.92
		side-on	1.82	2.50	3.53
EXAFS	$NpO_2(Succ)^-$/ $NpO_2(Succ)_2^{3-}$		1.83 ± 0.01	2.48 ± 0.02	2.83 ± 0.05

Theoretical approximations of the Gibbs free energies ΔG for the rearrangement of an end-on into a side-on coordinating ligand molecule according to scheme 1 support the side-on coordination for malonate and end-on coordination for succinate. The ΔG values are calculated according to equation (7).

$$\begin{aligned} \Delta G &= G_{end\text{-}on} - G_{side\text{-}on} \\ &= E_{g(end\text{-}on)} - E_{g(side\text{-}on)} + E_{vib(end\text{-}on)} - E_{vib(side\text{-}on)} + E_{solv(end\text{-}on)} - E_{solv(side\text{-}on)} \\ &= \Delta E_g + \Delta E_{vib} + \Delta E_{solv} \end{aligned} \qquad (7)$$

E_g are the ground state energies of the complexes calculated on MP2 level, E_{vib} considers thermodynamic corrections obtained from calculations of the vibrational modes and E_{solv} describes solvation effects which are calculated using COSMO. The results are listed in table 7.

Table 7: Gibbs free energies for the rearrangement of an end-on into a side-on coordinated ligand molecule.

complex	ΔE_g [kJ mol^{-1}]	ΔE_{vib} [kJ mol^{-1}]	ΔE_{solv} [kJ mol^{-1}]	ΔG [kJ mol^{-1}]
$NpO_2(Mal)^-$	11.14	-8.70	-4.35	-1.91
$NpO_2(Mal)_2^{3-}$	-44.02	-25.00	37.31	-31.70
$NpO_2(Succ)^-$	5.25	14.22	22.34	41.81
$NpO_2(Succ)_2^{3-}$	87.40	-43.67	-28.64	15.09

The calculated ΔG values show negative values for both $NpO_2(Mal)_n^{1-2n}$ complexes indicating an energetically preferred side-on coordination of malonate. In contrast, for both $NpO_2(Succ)_n^{1-n}$ complexes positive ΔG values are obtained indicating the preferred end-on coordination of succinate. Thus, the theoretical approximations of ΔG for an end-on into a side-on rearrangement of the ligand also confirm the results by EXAFS and ATR-FT-IR spectroscopy for both ligands.

4 Summary and Conclusions

The present work is a spectroscopic study on the complexation of Np(V) with malonate and succinate providing stability constants (log $\beta^0_n(T)$) and thermodynamic functions ($\Delta_r H^0_{n,m}$, $\Delta_r S^0_{n,m}$) as well as structural information on bond lengths and coordination modes of the ligands. For the determination of thermodynamic data the complexation is studied systematically as a function of the ligand concentration ($[Mal^{2-}]_{total}$, $[Succ^{2-}]_{total}$), ionic strength I_m (NaCl and $NaClO_4$ media) and temperature (20 – 85 °C) by absorption spectroscopy in the near infrared region. The formation of exclusively $NpO_2(Mal)_n^{1-2n}$ and $NpO_2(Succ)_n^{1-2n}$ (n = 1, 2) is observed at all studied conditions. The stoichiometry of the formed complexes is confirmed by slope analyses according to the law of mass action. Both complexation reactions are endothermic representing shifts of the chemical equilibrium towards the complexed Np(V) species with increasing temperature. This is also reflected by an increase of the stability constants. In case of malonate the log β^0_1(20 °C) = 3.31 ± 0.07 increases by 0.30 and log β^0_2(20 °C) = 3.90 ± 0.11 by 0.45. For $NpO_2(Succ)^-$ log β^0_1(20 °C) = 2.13 ± 0.15 increases by 0.43 logarithmic units. The formation of $NpO_2(Succ)_2^{3-}$ is only observed at temperatures higher than 50 °C. The integrated Van´t Hoff equation is used for the calculation of the standard reaction enthalpies and

standard reaction entropies as the stability constants correlate linearly with T^{-1}. The calculations reveal positive $\Delta_r H^0_{n,m}$ values for all reactions being driven by the gain of entropy.

Structural information about bond distances of the complexes and coordination modes of the ligands are obtained by EXAFS spectroscopy, ATR-FT-IR spectroscopy and quantum chemical calculations. The results reveal different coordination modes for malonate and succinate towards the Np(V) ion. For malonate a side-on coordination and the formation of six membered chelate rings is observed whereas succinate coordinates end-on via only one COO^- group. Thus, the formation of seven membered chelate rings in the equatorial plane of the Np(V) ion is energetically unfavourable.

The present work is a detailed spectroscopic study on thermodynamic functions for the complexation reactions of Np(V) with malonate and succinate revealing data at IUPAC reference state conditions. Thus, the present results are a valuable contribution to the thermodynamic database of actinides improving the scientific basis for describing the aquatic chemistry of actinide ions. Furthermore, extensive effort is made to clarify the structures of the formed complex species by application of EXAFS, ATR-FT-IR spectroscopy and quantum chemical calculations. The studied ligand systems serve as models to investigate the effect of steric hindrance in the coordination of Np(V) with macromolecular organic compounds. Thus, the derived data improve the knowledge of actinide-organic matter interaction at a molecular level.

Acknowledgements

All IR spectroscopic measurements were carried out at the *Institute of Resource Ecology* at the *Helmholtz-Zentrum Dresden–Rossendorf*. Dr. H. Foerstendorf is acknowledged for the helpful discussion regarding the IR spectroscopic data.

All absorption spectroscopic measurements were carried out at the *Institute for Nuclear Waste Disposal (INE)* at *Karlsruhe Institute of Technology (KIT)*. Dr. D. Fellhauer and Dr. M Altmaier are acknowledged for providing ^{237}Np and their experimental support.

The *KIT Institute for Beam Physics and Technology (IBPT)* is acknowledged for the operation of the storage ring, the Karlsruhe Research Accelerator (KARA), and provision of beamtime at the KIT light source.

The *European Synchrotron Radiation Facility* (ESRF) is acknowledged for the operation of the light source and provision of beamtime at the ROBL beamline.

This work is supported by the *German Federal Ministry for Economic Affairs and Energy (BMWI)* under contract 02E11415H and the *German Federal Ministry of Education and Research (BMBF)* under contract 02NUK039C.

Literature

1. Geckeis, H.; Röhlig, K.-J.; Mengel, K., Endlagerung radioaktiver Abfälle. *Chem. unserer Zeit* **2012,** *46* (5), 282-293.
2. Runde, W., The chemical interactions of actinides in the environment. *Los Alamos Science* **2000,** *26*, 392-411.
3. OECD; Agency, N. E., *Considering Timescales in the Post-closure Safety of Geological Disposal of Radioactive Waste*. 2009.
4. Gens, R.; Lalieux, P.; Preter, P. D.; Dierckx, A.; Bel, J.; Boyazis, J.-P.; Cool, W., The Second Safety Assessment and Feasibility Interim Report (SAFIR 2 Report) on HLW Disposal in Boom Clay: Overview of the Belgian Programme. *MRS Proceedings* **2011,** *807*, 917-924.
5. Oecd, N. E. A. *Safety of Geological Disposal of High-level and Long-lived Radioactive Waste in France* NUCLEAR ENERGY AGENCY ORGANISATION FOR ECONOMIC CO-OPERATION AND DEVELOPMENT: 2006.
6. Hoth, P.; Wirth, H.; Reinhold, K.; Bräuer, V.; Krull, P.; Feldrappe, H., Endlagerung radioaktiver Abfälle in tiefen geologischen Formationen Deutschlands–Untersuchung und Bewertung von Tongesteinsformationen. *BGR Bundesanstalt für Geowissenschaften und Rohstoffe, Hannover/Germany* **2007**.
7. NAGRA *Projekt Opalinuston – Synthese der geowissenschaftlichen Untersuchungsergebnisse, Entsorgungsnachweis für abgebrannte Brennelemente, verglaste hochaktive sowie langlebige mittelaktive Abfälle*; NAGRA Nationale Genossenschaft für die Lagerung radioaktiver Abfälle: Wettingen/Switzerland, 2002.
8. Mengel, K.; Röhlig, K.-J.; Geckeis, H., Endlagerung radioaktiver Abfälle. *Chem. unserer Zeit* **2012,** *46* (4), 208-217.
9. Röhlig, K.-J.; Geckeis, H.; Mengel, K., Endlagerung radioaktiver Abfälle. *Chem. unserer Zeit* **2012,** *46* (3), 140-149.
10. Hansen, F. D.; Leigh, C. D., *Salt disposal of heat-generating nuclear waste*. Sandia National Laboratories Albuquerque, NM: 2011.
11. Gaucher, E.; Robelin, C.; Matray, J. M.; Negral, G.; Gros, Y.; Heitz, J. F.; Vinsot, A.; Rebours, H.; Cassagnabere, A.; Bouchet, A., ANDRA underground research laboratory: interpretation of the mineralogical and geochemical data acquired in the Callovian-Oxfordian formation by investigative drilling. *Physics and Chemistry of the Earth* **2004,** *29* (1), 55-77.
12. Allen, T. R.; Stoller, R. E.; Yamanaka, S., *Comprehensive Nuclear Materials*. Elsevier: Radarweg 29, PO Box 211, 1000 AE Amsterdam, The Netherlands, 2012.
13. Courdouan, A.; Christl, I.; Meylan, S.; Wersin, P.; Kretzschmar, R., Isolation and characterization of dissolved organic matter from the Callovo–Oxfordian formation. *Appl. Geochem.* **2007,** *22* (7), 1537-1548.
14. Courdouan, A.; Christl, I.; Meylan, S.; Wersin, P.; Kretzschmar, R., Characterization of dissolved organic matter in anoxic rock extracts and in situ pore water of the Opalinus Clay. *Appl. Geochem.* **2007,** *22* (12), 2926-2939.
15. Thurman, E. M., *Organic Geochemistry of Natural Waters*. Springer, Dordrecht: 1985.
16. Wood, S. A., The aqueous geochemistry of the rare-earth elements: Critical stability constants for complexes with simple car□ylic acids at 25°C and 1 bar and their application to nuclear waste management. *Engineering Geology* **1993,** *34* (3-4), 229-259.
17. Hummel, W.; Anderegg, G.; Rao, L.; Puigdomenech, I.; Tochiyama, O., *Chemical Thermodynamics of Compounds and Complexes of U, Np, Pu, Am, Tc, Se, Ni and Zr with Selected Organic Ligands*. Elsvier B.V.: 2005.
18. Schnitzer, M.; Khan, S. U., *Humic substances in the environment*. M. Dekker: 1972.
19. Geckeis, H.; Lutzenkirchen, J.; Polly, R.; Rabung, T.; Schmidt, M., Mineral-water interface reactions of actinides. *Chem. Rev.* **2013,** *113* (2), 1016-62.

20. Choppin, G. R., The role of natural organics in radionuclide migration in natural aquifer systems. *Radiochimica Acta* **1992,** *58* (1), 113-120.
21. Hakanen, M.; Ervanne, H. *The influence of organic cement additives on radionuclide mobility A literature survey*; Finland, 2006; p 42.
22. Greenfield, B. F.; Ilett, D. J.; Ito, M.; McCrohon, R.; Heath, T. G.; Tweed, C. J.; Williams, S. J.; Yui, M., The Effect of Cement Additives on Radionuclide Solubilities. *Radiochimica Acta* **1998,** *82* (s1).
23. Skerencak-Frech, A.; Maiwald, M.; Trumm, M.; Fröhlich, D. R.; Panak, P. J., The complexation of Cm(III) with oxalate in aqueous solution at T = 20-90 degrees C: a combined TRLFS and quantum chemical study. *Inorg. Chem.* **2015,** *54* (4), 1860-8.
24. Skerencak-Frech, A.; Trumm, M.; Fröhlich, D. R.; Panak, P. J., Coordination and Thermodynamics of Trivalent Curium with Malonate at Increased Temperatures: A Spectroscopic and Quantum Chemical Study. *Inorg. Chem.* **2017,** *56* (17), 10172-10180.
25. Fröhlich, D. R.; Trumm, M.; Skerencak-Frech, A.; Panak, P. J., The Complexation of Cm(III) with Succinate Studied by Time-Resolved Laser Fluorescence Spectroscopy and Quantum Chemical Calculations. *Inorg. Chem.* **2016,** *55* (9), 4504-11.
26. Frohlich, D. R.; Koke, C.; Maiwald, M. M.; Chomyn, C.; Plank, J.; Panak, P. J., A spectroscopic study of the complexation reaction of trivalent lanthanides with a synthetic acrylate based PCE-superplasticizer. *Spectrochim Acta A Mol Biomol Spectrosc* **2019,** *207*, 270-275.
27. Fröhlich, D. R.; Maiwald, M. M.; Taube, F.; Plank, J.; Panak, P. J., A thermodynamical and structural study on the complexation of trivalent lanthanides with a polycarboxylate based concrete superplasticizer. *Dalton Trans* **2017,** *46* (12), 4093-4100.
28. Fellhauer, D.; Rothe, J.; Altmaier, M.; Neck, V.; Runke, J.; Wiss, T.; Fanghänel, T., Np(V) solubility, speciation and solid phase formation in alkaline $CaCl_2$ solutions. Part I: Experimental results. *Radiochimica Acta* **2016,** *104* (6), 355-379.
29. Müller, K.; Foerstendorf, H.; Tsushima, S.; Brendler, V.; Bernhard, G., Direct spectroscopic characterization of aqueous actinyl(VI) species: A comparative study of Np and U. *J. Phys. Chem. A* **2009,** *113* (24), 6626-6632.
30. Müller, K.; Foerstendorf, H.; Brendler, V.; Bernhard, G., Sorption of Np(V) onto TiO_2, SiO_2, and ZnO: An *in situ* ATR FT-IR spectroscopic study. *Environ. Sci. Technol.* **2009,** *43* (20), 7665-7670.
31. Glasoe, P. K.; Long, F. A., Use of glass electrodes to measure acidities in deuterium oxide. *J. Phys. Chem.* **1960,** *64* (1), 188-190.
32. Vasiliev, A. N.; Banik, N. L.; Marsac, R.; Fröhlich, D. R.; Rothe, J.; Kalmykov, S. N.; Marquardt, C. M., Np(v) complexation with propionate in 0.5-4 M NaCl solutions at 20-85 degrees C. *Dalton Trans* **2015,** *44* (8), 3837-44.
33. Altmaier, M.; Metz, V.; Neck, V.; Müller, R.; Fanghänel, T., Solid-liquid equilibria of Mg(OH)2(cr) and Mg2(OH)3Cl·4H2O(cr) in the system Mg-Na-H-OH-Cl-H2O at 25°C. *Geochim. Cosmochim. Acta* **2003,** *67* (19), 3595-3601.
34. A.Denecke, M.; Rothe, J.; Dardenne, K.; Blank, H.; Hormes, J., The INEBeamline for Actinide Research at ANKA. *Phys. Scr.* **2005**.
35. Rothe, J.; Butorin, S.; Dardenne, K.; Denecke, M. A.; Kienzler, B.; Loble, M.; Metz, V.; Seibert, A.; Steppert, M.; Vitova, T.; Walther, C.; Geckeis, H., The INE-Beamline for actinide science at ANKA. *Rev. Sci. Instrum.* **2012,** *83* (4), 043105.
36. Rothe, J.; Denecke, M. A.; Dardenne, K.; Fanghänel, T., The INE-Beamline for actinide research at ANKA. *Radiochimica Acta* **2006,** *94* (9-11).
37. Reich, T.; Bernhard, G.; Geipel, G.; Funke, H.; Hennig, C.; Roßberg, A.; Matz, W.; Schell, N.; Nitsche, H., The Rossendorf Beam Line ROBL – a dedicated experimental station for XAFS measurements of actinides and other radionuclides. *Radiochimica Acta* **2000,** *88* (9-11).
38. Matz, W.; Schell, N.; Bernhard, G.; Prokert, F.; Reich, T.; Claußner, J.; Oehme, W.; Schlenk, R.; Dienel, S.; Funke, H.; Eichhorn, F.; Betzl, M.; Pröhl, D.; Strauch, U.; Hüttig, G.; Krug, H.; Neumann, W.; Brendler, V.; Reichel, P.; Denecke, M. A.; Nitsche, H., ROBL – a CRG beamline for radiochemistry and materials research at the ESRF. *Journal of Synchrotron Radiation* **1999,** *6* (6), 1076-1085.
39. George, G. N.; Pickering, I. J., EXAFSPAK: A suite of computer programs for analysis of X-ray absorption spectra. *SSRL, Stanford* **1995**.

40. Newville, M., IFEFFIT : interactive XAFS analysis andFEFFfitting. *Journal of Synchrotron Radiation* **2001,** *8* (2), 322-324.
41. Ravel, B.; Newville, M., ATHENA, ARTEMIS, HEPHAESTUS: data analysis for X-ray absorption spectroscopy using IFEFFIT. *J Synchrotron Radiat* **2005,** *12* (Pt 4), 537-41.
42. Ankudinov, A. L.; Ravel, B.; Rehr, J. J.; Conradson, S. D., Real-space multiple-scattering calculation and interpretation of x-ray-absorption near-edge structure. *Physical Review B* **1998,** *58* (12), 7565-7576.
43. Rehr, J. J.; Kas, J. J.; Prange, M. P.; Sorini, A. P.; Takimoto, Y.; Vila, F., Ab initio theory and calculations of X-ray spectra. *Comptes Rendus Physique* **2009,** *10* (6), 548-559.
44. Bombieri, G.; Benetollo, F.; Del Pra, A.; Rojas, R., Structural studies on the actinide carboxylates—IV The crystal and molecular structure of succinate dioxouranium(VI) monohydrate. *J. Inorg. Nucl. Chem.* **1979,** *41* (2), 201-203.
45. Rojas, R. M.; Del Pra, A.; Bombieri, G.; Benetollo, F., Structural studies on actinides carboxylates—V[1]. *J. Inorg. Nucl. Chem.* **1979,** *41* (4), 541-545.
46. Furche, F.; Ahlrichs, R.; Hättig, C.; Klopper, W.; Sierka, M.; Weigend, F., Turbomole. *Wiley Interdisciplinary Reviews: Computational Molecular Science* **2014,** *4* (2), 91-100.
47. Becke, A. D., A new mixing of Hartree–Fock and local density-functional theories. *The Journal of Chemical Physics* **1993,** *98* (2), 1372.
48. Küchle, W.; Dolg, M.; Stoll, H.; Preuss, H., Energy-adjusted pseudopotentials for the actinides. Parameter sets and test calculations for thorium and thorium monoxide. *The Journal of Chemical Physics* **1994,** *100* (10), 7535.
49. Weigend, F.; Häser, M., RI-MP2: first derivatives and global consistency. *Theor. Chem. Acc.* **1997,** *97* (1-4), 331-340.
50. Weigend, F.; Häser, M.; Patzelt, H.; Ahlrichs, R., RI-MP2: optimized auxiliary basis sets and demonstration of efficiency. *Chemical Physics Letters* **1998,** *294* (1-3), 143-152.
51. Klamt, A.; Schüürmann, G., COSMO: a new approach to dielectric screening in solvents with explicit expressions for the screening energy and its gradient. *Journal of the Chemical Society, Perkin Transactions 2* **1993,** (5), 799.
52. Neck, V.; Fanghänel, T.; Rudolph, G.; Kim, J. I., Thermodynamics of Neptunium(Y) in Concentrated Salt Solutions: Chloride Complexation and Ion Interaction (Pitzer) Parameters for the NpO_2^+ Ion. *Radiochimica Acta* **1995,** *69* (1), 39-47.
53. Maiwald, M. M.; Fellhauer, D.; Skerencak-Frech, A.; Panak, P. J., The complexation of neptunium(V) with fluoride at elevated temperatures: Speciation and thermodynamics. *Appl. Geochem.* **2019,** *104*, 10-18.
54. Maiwald, M. M.; Sittel, T.; Fellhauer, D.; Skerencak-Frech, A.; Panak, P. J., Thermodynamics of neptunium(V) complexation with sulfate in aqueous solution. *The Journal of Chemical Thermodynamics* **2018,** *116*, 309-315.
55. Hagan, P. G.; Cleveland, J. M., The absorption spectra of neptunium ions in perchloric acid solution. *J. Inorg. Nucl. Chem.* **1966,** *28* (12), 2905-2909.
56. Maiwald, M. M.; Skerencak-Frech, A.; Panak, P. J., The complexation and thermodynamics of neptunium(V) with acetate in aqueous solution. *New J. Chem.* **2018,** *42* (10), 7796-7802.
57. Zhang, Z.; Yang, Y.; Liu, G.; Luo, S.; Rao, L., Effect of temperature on the thermodynamic and spectroscopic properties of Np(v) complexes with picolinate. *RSC Advances* **2015,** *5* (92), 75483-75490.
58. Yang, Y.; Zhang, Z.; Liu, G.; Luo, S.; Rao, L., Effect of temperature on the complexation of NpO_2^+ with benzoic acid: Spectrophotometric and calorimetric studies. *The Journal of Chemical Thermodynamics* **2015,** *80*, 73-78.
59. Skerencak, A.; Panak, P. J.; Hauser, W.; Neck, V.; Klenze, R.; Lindqvist-Reis, P.; Fanghanel, T., TRLFS study on the complexation of Cm(III) with nitrate in the temperature range from 5 to 200 degrees C. *Radiochimica Acta* **2009,** *97* (8), 385-393.
60. Skerencak, A.; Panak, P. J.; Fanghänel, T., Complexation and thermodynamics of Cm(III) at high temperatures: the formation of $[Cm(SO_4)_n]^{3-2n}$ (n = 1, 2, 3) complexes at T = 25 to 200°C. *Dalton Transaction* **2013,** *42*, 542-549.

61. Alderighi, L.; Gans, P.; Ienco, A.; Peters, D.; Sabatini, A.; Vacca, A., Hyperquad simulation and speciation (HySS): a utility program for the investigation of equilibria involving soluble and partially soluble species. *Coord. Chem. Rev.* **1999,** *184* (1), 311-318.
62. Puigdomènech, I.; Rard, J. A.; Plyasunov, A. V.; Grenthe, I.; Seine-st Germain, L.; Des Îles, B. *Temperature corrections to thermodynamic data and enthalpy calculations*; Le Seine-St. Germain 12, Bd. des Îles, F-92130 Issy-les-Moulineaux, France, 1999.
63. Kettler, R. M.; Palmer, D. A.; Wesolowski, D. J., Dissociation quotients of succinic acid in aqueous sodium chloride media to 225° C. *J. Solution Chem.* **1995,** *24* (1), 65-87.
64. Kettler, R. M.; Wesolowski, D. J.; Palmer, D. A., Dissociation quotients of malonic acid in aqueous sodium chloride media to 100 C. *J. Solution Chem.* **1992,** *21* (8), 883-900.
65. Smith, R.; Martell, A.; Motekaitis, R., *NIST standard reference database 46 ver. 6*. 2004.
66. Daniele, P. G.; Rigano, C.; Sammartano, S., The formation of proton and alkali-metal complexes with ligands of biological intrest in aqueous solution. Thermodynamics of H$^+$, Na$^+$ and K$^+$ -oxalate complexes. *Thermochim. Acta* **1981,** *46*, 103-116.
67. Daniele, P. G.; Rigano, C.; Sammartano, S., The formation of proton and alkali metal complexes with ligands of biological interest in aqueous solution. Thermodynamics of Li+, Na+ and K+-dicarboxylate complex formation. *Thermochim. Acta* **1983,** *62* (1), 101-112.
68. Hummel, W.; Puigdomenech, I.; Rao, L.; Tochiyama, O., Thermodynamic data of compounds and complexes of U, Np, Pu and Am with selected organic ligands. *C. R. Chim.* **2007,** *10*, 948-958.
69. Martell, A. E. a. S., R.M. and Motekaitis, R.J., *NIST standard reference database 46 version 8.0: NIST critically selected stability constants of metal complexes*. U.S. Department of Commerce,Technology Administration, National Institute of Standards and Technology, Standard Reference Data Program: Gaithersburg, MD, 2004.
70. Maiwald, M. M.; Trumm, M.; Dardenne, K.; Rothe, J.; Skerencak-Frech, A.; Panak, P. J.; Speciation, thermodynamics and structure of Np(V) oxalate in aqueous solution. *Dalton Trans* 2020, **49**, 13359-13371.
71. Fröhlich, D. R.; Skerencak-Frech, A.; Panak, P. J., A spectroscopic study on the formation of Cm(III) acetate complexes at elevated temperatures. *Dalton Trans* **2014,** *43* (10), 3958-65.
72. Maiwald, M. M.; Dardenne, K.; Rothe, J.; Skerencak-Frech, A.; Panak, P. J., Thermodynamics and Structure of Neptunium(V) Complexes with Formate. Spectroscopic and Theoretical Study. *Inorg. Chem.* **2020,** *59* (9), 6067-6077.
73. Guillaumont, R.; Fanghänel, T.; Neck, V.; Fuger, J.; Palmer, D. A., *Update on the Chemical Thermodynamics of Uranium, Neptunium, Plutonium, Americium and Technetium*. Elsvier B.V.: 2003.
74. Kettler, R. M.; Palmer, D. A.; Wesolowski, D. J., Dissociation quotients of succinic acid in aqueous sodium chloride media to 225°C. *J. Solution Chem.* **1995,** *24* (1), 65-87.
75. Hug, S. J.; Bahnemann, D., Infrared spectra of oxalate, malonate and succinate adsorbed on the aqueous surface of rutile, anatase and lepidocrocite measured with in situ ATR-FTIR. *Journal of Electron Spectroscopy and Related Phenomena* **2006,** *150* (2-3), 208-219.
76. Deacon, G. B.; Phillips, R. J., Relationships between the carbon-oxygen stretching frequencies of carboxylato complexes and the type of carboxylate coordination. *Coord. Chem. Rev.* **1980,** *33* (3), 227-250.
77. Jones, L. H.; Penneman, R. A., Infrared Spectra and Structure of Uranyl and Transuranium(V) and(VI) Ions in Aqueous Perchloric Acid Solution. *J. Chem. Phys.* **1953,** *21* (3), 542-544.
78. Allen, P. G.; Bucher, J. J.; Shuh, D. K.; Edelstein, N. M.; Reich, T., Investigation of Aquo and Chloro Complexes of UO22+, NpO2+, Np4+, and Pu3+by X-ray Absorption Fine Structure Spectroscopy. *Inorg. Chem.* **1997,** *36* (21), 4676-4683.
79. Takao, K.; Takao, S.; Scheinost, A. C.; Bernhard, G.; Hennig, C., Complex formation and molecular structure of neptunyl(VI) and -(V) acetates. *Inorg. Chem.* **2009,** *48* (18), 8803-10.